



HHS Public Access

Author manuscript

Biochem Biophys Res Commun. Author manuscript; available in PMC 2018 September 02.

Published in final edited form as:

Biochem Biophys Res Commun. 2017 September 02; 490(4): 1226–1231. doi:10.1016/j.bbrc.2017.06.195.

Regulation of calcium release from the endoplasmic reticulum by the serine hydrolase ABHD2

Bogeon Yun^a, HeeJung Lee^a, Roger Powell^{b,1}, Nichole Reisdorph^{b,1}, Heather Ewing^{c,d}, Michael H. Gelb^{c,d}, Ku-Lung Hsu^e, Benjamin F. Cravatt^f, and Christina C. Leslie^{a,*}

^aDepartment of Pediatrics, National Jewish Health, Denver, CO 80206 USA

^bDepartment of Immunology, National Jewish Health, Denver, CO 80206 USA

^cDepartment of Chemistry, University of Washington, Seattle, WA 98195 USA

^dDepartment of Biochemistry, University of Washington, Seattle, WA 98195 USA

^eDepartment of Chemistry, University of Virginia, Charlottesville, VA 22904 USA

^fDepartment of Chemical Physiology, The Skaggs Institute for Chemical Biology, The Scripps Research Institute, La Jolla, CA 92037 USA

Abstract

The serine hydrolase inhibitors pyrrophenone and KT195 inhibit cell death induced by A23187 and H₂O₂ by blocking the release of calcium from the endoplasmic reticulum and mitochondrial calcium uptake. The effect of pyrrophenone and KT195 on these processes is not due to inhibition of their known targets, cytosolic phospholipase A₂ and α/β -hydrolase domain-containing (ABHD) 6, respectively, but represent off-target effects. To identify targets of KT195, fibroblasts were treated with KT195-alkyne to covalently label protein targets followed by click chemistry with biotin azide, enrichment on streptavidin beads and tryptic peptide analysis by mass spectrometry. Although several serine hydrolases were identified, α/β -hydrolase domain-containing 2 (ABHD2) was the only target in which both KT195 and pyrrophenone competed for binding to KT195-alkyne. ABHD2 is a serine hydrolase with a predicted transmembrane domain consistent with its pull-down from the membrane proteome. Subcellular fractionation showed localization of ABHD2 to the endoplasmic reticulum but not to mitochondria or mitochondrial-associated membranes. Knockdown of ABHD2 with shRNA attenuated calcium release from the endoplasmic reticulum, mitochondrial calcium uptake and cell death in fibroblasts stimulated with A23187. The results describe a novel mechanism for regulating calcium transfer from the endoplasmic reticulum to mitochondria that involves the serine hydrolase ABHD2.

Keywords

calcium; endoplasmic reticulum; mitochondria; serine hydrolase; pyrrophenone; ABHD2; cell death; H₂O₂

*Corresponding author. National Jewish Health, Department of Pediatrics, 1400 Jackson St., Denver, CO 80206 USA.

¹Present Address. Skaggs School of Pharmacy and Pharmaceutical Sciences, University of Colorado, Aurora, CO 80045 USA

1. Introduction

Calcium signals regulate many processes such as proliferation, secretion, metabolism and transcription [1]. Cytosolic calcium concentration is finely regulated through a number of uptake and efflux mechanisms. Inositol trisphosphate (IP₃) production stimulates calcium release from the endoplasmic reticulum (ER) through IP₃ receptors (IP₃R), which is transferred to mitochondria through specialized contact sites, mitochondrial-associated membranes (MAM) [2–4]. Mitochondrial calcium uptake regulates bioenergetics and ATP production. However, during cell injury and ER stress, excess calcium is transferred through the IP₃R/MAM pathway into mitochondria that together with reactive oxygen species (ROS) production initiates cell death pathways, including intrinsic apoptosis and necrosis [5, 6]. Intrinsic apoptosis is triggered by injurious agents (ROS, genotoxic agents, irradiation) and involves caspase 9 activation, calcium mobilization, and mitochondrial outer membrane permeabilization [7]. Necrosis was historically considered “accidental” from exposure to harsh treatments, however, several regulated necrotic cell death pathways have now been described including cyclophilin D (CyD)-mediated necrosis that involves mitochondrial calcium overload and production of ROS that trigger opening of the mitochondrial permeability transition pore (MPTP) [8–10]. This occurs in response to extreme insults such as exposure to environmental toxicants, toxic drugs, during ischemia/reperfusion injury (myocardial infarction, stroke, heart failure), neurological disorders (Parkinson’s) and muscular dystrophies [11–16]. Calcium ionophores and H₂O₂ are classical inducers of CyD-dependent necrosis, which is blocked by the CyD inhibitor cyclosporin A [6, 17]. Necrosis is characterized by irreversible MPTP opening, mitochondria swelling, depolarization, ATP depletion, and plasma membrane rupture [15, 16].

We reported that serine hydrolase inhibitors, pyrrophenone and the triazolurea inhibitor KT195 inhibit CyD-dependent necrotic cell death in lung fibroblasts by blocking ER calcium release, mitochondrial calcium uptake and MPTP formation [18–22]. Pyrrophenone and KT195 do not block cell death by inhibiting their known targets, cytosolic phospholipase A₂ (cPLA₂α) and α/β-hydrolase domain-containing 6 (ABHD6), respectively but by off-target effects [18–20]. They also inhibit ER calcium release triggered by receptor stimulation with ATP and serum, which act by increasing IP₃ production [22]. The results suggest that the inhibitors target a serine hydrolase that regulates ER calcium release through IP₃R that is transferred to mitochondria. Using click chemistry-activity based protein profiling we identified the serine hydrolase, ABHD2, as the likely target of the inhibitors. ABHD proteins are a large family (~19 members) of enzymes with an α/β-hydrolase fold containing a catalytic triad (nucleophile-carboxylic acid-histidine) with GX SXG as the consensus lipase serine nucleophile motif [23]. Many ABHD enzymes are predicted to be involved in lipid metabolism but are poorly characterized including ABHD2, which is widely expressed in tissues and highly conserved evolutionarily [24].

2. Materials and Methods

2.1. Cells

Primary mouse lung fibroblasts (MLF) from cPLA₂α^{-/-} mice and MLF immortalized with SV40 were used for all experiments [18, 25].

2.2. Chemical proteomics activity-based protein profiling

Chemical proteomics using alkyne-tagged KT195 was used to identify targets of the serine hydrolase inhibitor in IMLF by click chemistry-activity based protein profiling [26]. IMLF (~10–15, 15 cm plates/sample) were treated with KT195-alkyne (5 μ M) for 1 h to covalently label protein targets. Membrane and soluble proteomes were prepared and samples (~1 mg protein/0.5 ml) incubated with biotin-azide reporter for covalent attachment to KT195-alkyne-labeled targets using Cu(I)-catalyzed click chemistry as described in detail [20, 27]. Biotin-azide-tagged targets were enriched using Immunopure immobilized streptavidin beads followed by on-bead reduction, alkylation and digestion with trypsin [27]. Proteomes from fibroblasts not treated with KT195-alkyne were included as controls to eliminate false positives due to non-specific bead binding. Peptides were eluted and desalted with C18 spin columns (ThermoFisher scientific), dried, and then solubilized with 3% acetonitrile and 0.1% formic acid for mass spectrometry.

Peptides were analyzed via LC/MS/MS on an Agilent QTOF (model 6550) mass spectrometer. An HPLC chip (Agilent G4240–62006) was used which consisted of a 40 nL enrichment column and a 150 mm \times 75 μ m analytical column. Nano pump buffer A (0.1% formic acid), buffer B (90% acetonitrile, 10% HPLC grade water, 0.1% formic acid) and loading pump buffer (3% acetonitrile in 97% HPLC grade water with 0.1% formic acid) were used. Samples were run with a 23 min LC/MS/MS method using a gradient from 3–30% buffer B over 0–18 min. Raw LC/MS/MS data were searched using the Agilent Spectrum Mill search engine and a Swissprot mouse database. “Peak picking” was performed within SpectrumMill with the following parameters: signal-to-noise was set at 15:1 and variable modifications searched for oxidized methionine and deamidated asparagine, maximum charge state for peptides was set at 7, precursor mass tolerance of 20 PPM and product mass tolerance of 50 PPM. Matched peptides were filtered with a score >6 and a Scored Peak Intensity of $>60\%$.

In some experiments membrane proteomes were prepared from IMLF treated with KT195-alkyne and then click chemistry carried out using rhodamine-azide (100 μ M). The reactions were terminated with SDS sample buffer, and proteins separated on 10% polyacrylamide gels. Rhodamine-labeled targets were visualized by in-gel fluorescence scanning as described [18].

2.3. Subcellular fractionation and Western blotting

A protocol designed to isolate MAM, mitochondria and ER was used for subcellular fractionation of IMLF using 10–15, 15 cm dishes ($\sim 7 \times 10^6$ cells/dish) as described [28]. Western blot analysis was used to detect protein markers in the subcellular fractions (10 μ g/lane) using the following antibodies: anti-long-chain fatty-acid CoA synthase (1:2500, GeneTex) for MAM; anti-oxidative phosphorylation complex V (1:1000, ThermoFisher Scientific) for mitochondria; anti-GRP78 (1:1000, abcam) for ER; anti-MEK1/2 (1:1000, Cell Signaling Technology) for cytosol and anti-ABHD2 (1:2000, Proteintech).

2.3. Silencing of ABHD2

Lentiviruses containing ABHD2 shRNA (clone TRCN0000121483, Functional Genomics Facility, University of Colorado) or empty vector (control) were generated using 2nd Generation Packaging Mix and Lentifectin according to the manufacturer's protocol (abm). After transfection with lentiviruses, stable IMLF cell lines were selected using puromycin (10 µg/ml). Clones isolated by limiting dilution were screened for levels of ABHD2 protein on Western blots and mRNA by real-time PCR (probe Mm00502098_m1, ThermoFisher Scientific), as previously described [18].

2.4. Live-cell calcium imaging

Imaging of ER and mitochondrial calcium following stimulation with A23187 (1 µg/ml) was carried out in control and ABHD2 knockdown IMLF expressing calcium-measuring organelle-entrapped protein indicators (CEPIA) that target to ER (G-CEPIAer) or mitochondria (CEPIA2mt) as described [22, 29].

2.5. Cell death assays

MLF were cultured in DMEM containing 1% FBS for 16 h and then treated with and without inhibitors for 30 min followed by stimulation with H₂O₂ or staurosporine for 1–6 h. For determining necrotic cell death, lactate dehydrogenase (LDH) released into the culture medium was measured using CytoTox ONE homogeneous membrane integrity assay kit as described [18]. For apoptosis, MLF were washed with PBS and labeled with Alexa 488-annexin V, propidium iodide and DAPI (ThermoFisher scientific), or incubated with caspase 3/7 activity assay reagents (Cell Technology), according to the manufacturer. MLF labeled with annexin V, propidium iodide and DAPI were imaged using a Marianas 200 spinning disk confocal microscope using excitation/emission 405/450, 488/525 and 561/617 nm, respectively and counted. For determining caspase 3/7 activity, fluorescence from cells in 96-well microplates was measured using a Wallac Victor² 1420 Multilabel Counter (488/525 nm excitation/emission).

3. Results

3.1 Serine hydrolase inhibitors block H₂O₂ induced apoptosis and necrosis

Pyrrophenone and KT195 inhibit necrotic cell death but we had not tested their effect on caspase-dependent apoptosis [18]. H₂O₂ induces necrosis at high concentrations (~1 mM) but induces caspase-mediated apoptosis at nM concentrations [17, 30–32]. H₂O₂ at 1 mM was the most effective concentration at stimulating LDH release (necrosis) from MLF (Fig. 1A), but did not induce caspase activation (Fig. 1B). Lower concentrations of H₂O₂ (0.05–0.2 µM) induced apoptosis (caspase activation and annexin V staining) (Fig. 1B & C) but not necrosis (propidium iodide staining) (Fig. 1C), as observed for staurosporine, a known inducer of apoptosis (Fig. 1B & C). The caspase inhibitor zVAD blocked apoptosis induced by staurosporine and 50 µM H₂O₂ (Fig. 1D & E). Pyrrophenone and KT195, and other inhibitors of MPTP formation (the CaMKII inhibitor KN93 and CyD inhibitor cyclosporin A), blocked apoptosis induced by H₂O₂ but not by staurosporine (Fig. 1D & E). The results suggest that the target of pyrrophenone and KT195 regulates apoptosis and necrosis that

involves CaMKII activation and CyD-dependent MPTP formation but not apoptosis induced by staurosporine that is independent of MPTP formation [17, 18, 32].

3.2 Identification of ABHD2 as the target of pyrrophenone and KT195

Click chemistry involves metal catalyzed cycloaddition between azides and terminal alkynes to functionally characterize enzymes in complex biological systems and is useful for identifying low abundance targets [33, 34]. KT195-alkyne was used as a chemical probe to covalently label the active serine hydrolase target(s) in IMLF. KT195 was chosen since it inhibits by covalent, irreversible carbamylation of active site serines [20, 35]. Pyrrophenone is a slowly reversible inhibitor that may not form a long-lived complex with the target protein [19]. KT195-alkyne inhibited necrotic cell death (LDH release) induced by A23187 with an $IC_{50} \sim 1.5 \mu M$, comparable to non-substituted KT195 ($IC_{50} 0.7 \mu M$) (Fig. 2A) [18]. To confirm labeling of KT195-alkyne to the known target, ABHD6, IMLF were treated with KT195-alkyne and click chemistry carried out with membrane proteomes using Rhodamine-azide. Targets were visualized in polyacrylamide gels by fluorescence scanning (Fig. 2B) [18, 21]. The strongest labeled band (35 kDa) corresponds to ABHD6 the known target of KT195 and another major band at 47 kDa was also evident.

To identify targets of the inhibitors IMLF were treated with KT195-alkyne and click chemistry carried out in membrane and soluble proteomes using biotin azide, followed by pull-down with streptavidin beads and LC/MS analysis of tryptic peptides [26]. Several of the candidates were serine hydrolases, and the greatest number of tryptic peptides identified was from the positive control, ABHD6 (Table 1). To narrow down the targets, competition experiments were performed by pre-treating IMLF with $10 \mu M$ KT195 (Exp 2) or $10 \mu M$ pyrrophenone (Exp 3) prior to incubating with KT195-alkyne. A criterion for considering a protein target for further study was competitive inhibition by both KT195 and pyrrophenone since they have very similar effects. KT195 (Exp 2), but not pyrrophenone (Exp 3), blocked KT195-alkyne binding to the positive control ABHD6 since no ABHD6 tryptic peptides were recovered. ABHD2 was the only serine hydrolase in which both KT195 and pyrrophenone competed for binding to KT195-alkyne (Table 1). The ABHD2 peptide found in experiments 1 and 3 was (K)KPQSLETDLSR(L), and the three ABHD2 peptides identified in experiment 2 were (K)EYIPPLIWGK(S); (K)SGHIQTALYGK(M); (R)TFVDYAQK(N). ABHD2 was identified in the membrane proteome but not in pull downs from the soluble fraction. It is predicted to have a single transmembrane domain with a molecular weight of 48 kDa (Fig. 3A), the molecular weight of a major band labeled by rhodamine-azide in proteomes of IMLF treated with KT195-alkyne (see Fig. 1B).

3.3 Subcellular localization of ABHD2

Subcellular fractionation of IMLF showed ABHD2 localization to ER but not MAM or mitochondria [28] (Fig. 3B). We confirmed the specific localization of the MAM protein fatty acid CoA ligase 4 (FACL4) and the mitochondria protein oxidative phosphorylation complex V (OxPhos) [4]. MEK1/2 was found primarily in cytosol and mitochondria, and GRP78 in both ER and mitochondria but not MAM [36, 37].

3.4 Effect of ABHD2 knockdown

IMLF transfected with ABHD2 shRNA showed 72% knockdown of ABHD2 mRNA compared to control cells, and less ABHD2 in Western blots (Fig. 4, inset). When treated with A23187 to induce cell death, the ABHD2 knockdown IMLF clone exhibited less LDH release (Fig. 4A), less ER calcium release (Fig. 4B) and less mitochondrial calcium uptake (Fig. 4C) compared to control cells implicating a role for ABHD2 in these processes.

4. Discussion

The results suggest that pyrrophenone and KT195 block ER calcium release and cell death by targeting the serine nucleophile in ABHD2. Pyrrophenone inhibits via formation of a hemiketal between its ketone carbonyl and the active site serine [38–40]. When the ketone is reduced to a secondary alcohol it loses the ability to inhibit cell death [18]. KT195 inhibits by covalent, irreversible carbamoylation of the active site serine. We have uncovered a novel mechanism involving the serine hydrolase ABHD2 for regulating ER calcium release [18, 22].

ABHD enzymes hydrolyze a variety of substrates including medium-chain and oxidatively-truncated phospholipids (ABHD3), N-acyl-phosphatidylethanolamine (NAPE) and lysoNAPE (ABHD4), 2-arachidonoyl-glycerol (ABHD6, ABHD12), phosphatidylserine (ABHD16A), lyso-phosphatidylserine (ABHD12) and palmitoylated proteins (ABHD17) suggesting diverse metabolic functions *in vivo* [23, 41–44]. The residues S207/D345/H376 form the catalytic triad of ABHD2, which also has a conserved acyltransferase motif at residues H120-XXXX-D125 [23] (Fig. 3A). Affinity purified His-tagged ABHD2 has esterase activity against p-nitrophenyl conjugated substrates (acetate, butyrate and palmitate) and triacylglycerol lipase activity *in vitro* although little is known about the substrates hydrolyzed by ABHD2 *in vivo* [45]. ABHD2 plays a specialized role in sperm flagella where it hydrolyzes 2-arachidonoylglycerol, a negative regulator of sperm-specific calcium channel CatSper, leading to calcium mobilization and sperm activation [46].

We reported that pyrrophenone blocks ER calcium release induced by receptor stimulation but not by thapsigargin suggesting that ABHD2 regulates IP₃-mediated ER calcium release pathway that couples to mitochondrial calcium uptake, and not pathways that control basal calcium release [22]. A study that directly relates to our findings showed that ABHD2 knockdown blocks hepatitis B virus propagation [47]. Although the authors provided no mechanism, hepatitis B virus replication is regulated by ER calcium release through IP₃R, mitochondrial calcium uptake and MPTP formation [48, 49]. Identification of ABHD2 as the target of pyrrophenone and KT195 implicates this poorly characterized enzyme as a critical player in regulating ER calcium release. Understanding the biochemical properties and function of ABHD2 will provide new insight into a previously unrecognized regulatory step in a fundamental process that is essential for cell function and that promotes cell death. Serine hydrolases are a large (~250) diverse class of biologically important enzymes (lipases, esterases, thioesterases, proteases, amidases), and a number of inhibitors that target these enzymes have been approved for clinical use [50]. However, the enzymatic substrates and biological functions of many serine hydrolases are unknown, and development of inhibitors is essential for their characterization with potential for therapeutic use. The

development of specific small molecule cell permeable ABHD2 inhibitors will be important for understanding its mechanistic role in regulating these important processes [50, 51].

Acknowledgments

The work was funded by the National Institutes of Health Grant ES025015 to CCL.

Abbreviations

ABHD	α/β -hydrolase domain-containing
cPLA₂α	cytosolic phospholipase A ₂ α
CEPIA	calcium-measuring organelle-entrapped protein indicators
CyD	cyclophilin D
ER	endoplasmic reticulum
IP₃	inositol trisphosphate
IP₃R	IP ₃ receptors
LDH	lactate dehydrogenase
MAM	mitochondrial-associated membranes
MLF	mouse lung fibroblasts
IMLF	immortalized MLF
MPTP	mitochondrial permeability transition pore
ROS	reactive oxygen species

References

1. Berridge MJ. The versatility and complexity of calcium signalling. *Novartis Found Symp.* 2000; 239:52–64. discussion 64–57, 150–159.
2. Berridge MJ. Inositol trisphosphate and calcium signaling. *Ann N Y Acad Sci.* 1995; 766:31–43. [PubMed: 7486679]
3. Rizzuto R, Pinton P, Carrington W, Fay FS, Fogarty KE, Lifshitz LM, Tuft RA, Pozzan T. Close contacts with the endoplasmic reticulum as determinants of mitochondrial Ca²⁺ responses. *Science.* 1998; 280:1763–1766. [PubMed: 9624056]
4. Vance JE. MAM (mitochondria-associated membranes) in mammalian cells: Lipids and beyond. *Biochim Biophys Acta.* 2013;595–609.
5. La Rovere RM, Roest G, Bultynck G, Parys JB. Intracellular Ca²⁺ signaling and Ca²⁺ microdomains in the control of cell survival, apoptosis and autophagy. *Cell Calcium.* 2016; 60:74–87. [PubMed: 27157108]
6. Zhivotovsky B, Orrenius S. Calcium and cell death mechanisms: a perspective from the cell death community. *Cell Calcium.* 2011; 50:211–221. [PubMed: 21459443]
7. Tajeddine N. How do reactive oxygen species and calcium trigger mitochondrial membrane permeabilisation? *Biochim Biophys Acta.* 2016; 1860:1079–1088. [PubMed: 26922832]

8. Vanden Berghe T, Linkermann A, Jouan-Lanhouet S, Walczak H, Vandenabeele P. Regulated necrosis: the expanding network of non-apoptotic cell death pathways. *Nat Rev Mol Cell Biol.* 2014; 15:135–147. [PubMed: 24452471]
9. Lemasters JJ, Theruvath TP, Zhong Z, Nieminen AL. Mitochondrial calcium and the permeability transition in cell death. *Biochim Biophys Acta.* 2009; 1787:1395–1401. [PubMed: 19576166]
10. Giorgio V, von Stockum S, Antoniel M, Fabbro A, Fogolari F, Forte M, Glick GD, Petronilli V, Zoratti M, Szabo I, Lippe G, Bernardi P. Dimers of mitochondrial ATP synthase form the permeability transition pore. *Proc Natl Acad Sci USA.* 2013; 110:5887–5892. [PubMed: 23530243]
11. Eltzschig HK, Eckle T. Ischemia and reperfusion—from mechanism to translation. *Nat Med.* 2011; 17:1391–1401. [PubMed: 22064429]
12. Kamel F. Epidemiology. Paths from pesticides to Parkinson's. *Science.* 2013; 341:722–723. [PubMed: 23950519]
13. Xiong N, Long X, Xiong J, Jia M, Chen C, Huang J, Ghoorah D, Kong X, Lin Z, Wang T. Mitochondrial complex I inhibitor rotenone-induced toxicity and its potential mechanisms in Parkinson's disease models. *Crit Rev Toxicol.* 2012; 42:613–632. [PubMed: 22574684]
14. Bernardi P, Bonaldo P. Mitochondrial dysfunction and defective autophagy in the pathogenesis of collagen VI muscular dystrophies. *Cold Spring Harb Perspect Biol.* 2013; 5:a011387. [PubMed: 23580791]
15. Baines CP. The mitochondrial permeability transition pore and the cardiac necrotic program. *Pediatr Cardiol.* 2011; 32:258–262.
16. Halestrap AP. A pore way to die: the role of mitochondria in reperfusion injury and cardioprotection. *Biochem Soc Transact.* 2010; 38:841–860.
17. Nakagawa T, Shimizu S, Watanabe T, Yamaguchi O, Otsu K, Yamagata H, Inohara H, Kubo T, Tsujimoto Y. Cyclophilin D-dependent mitochondrial permeability transition regulates some necrotic but not apoptotic cell death. *Nature.* 2005; 434:652–658. [PubMed: 15800626]
18. Yun B, Lee H, Ghosh M, Cravatt BF, Hsu KL, Bonventre JV, Ewing H, Gelb MH, Leslie CC. Serine hydrolase inhibitors block necrotic cell death by preventing calcium overload of the mitochondria and permeability transition pore formation. *J Biol Chem.* 2014; 289:1491–1504. [PubMed: 24297180]
19. Ono T, Yamada K, Chikazawa Y, Ueno M, Nakamoto S, Okuno T, Seno K. Characterization of a novel inhibitor of cytosolic phospholipase A₂, pyrrophenone. *Biochem J.* 2002; 363:727–735. [PubMed: 11964173]
20. Hsu KL, Tsuboi K, Adibekian A, Pugh H, Masuda K, Cravatt BF. DAGLβ inhibition perturbs a lipid network involved in macrophage inflammatory responses. *Nat Chem Biol.* 2012; 8:999–1007. [PubMed: 23103940]
21. Hsu KL, Tsuboi K, Chang JW, Whitby LR, Speers AE, Pugh H, Cravatt BF. Discovery and optimization of piperidyl-1,2,3-triazole ureas as potent, selective, and in vivo-active inhibitors of alpha/beta-hydrolase domain containing 6 (ABHD6). *J Med Chem.* 2013; 56:8270–8279. [PubMed: 24152295]
22. Yun B, Lee H, Ewing H, Gelb MH, Leslie CC. Off-target effect of the cPLA₂α inhibitor pyrrophenone: Inhibition of calcium release from the endoplasmic reticulum. *Biochem Biophys Res Commun.* 2016; 479:61–66. [PubMed: 27620490]
23. Lord CC, Thomas G, Brown JM. Mammalian alpha beta hydrolase domain (ABHD) proteins: Lipid metabolizing enzymes at the interface of cell signaling and energy metabolism. *Biochim Biophys Acta.* 2013; 1831:792–802. [PubMed: 23328280]
24. Edgar AJ, Polak JM. Cloning and tissue distribution of three murine alpha/beta hydrolase fold protein cDNAs. *Biochem Biophys Res Commun.* 2002; 292:617–625. [PubMed: 11922611]
25. Stewart A, Ghosh M, Spencer DM, Leslie CC. Enzymatic properties of human cytosolic phospholipase A₂g. *J Biol Chem.* 2002; 277:29526–29536. [PubMed: 12039969]
26. Chang JW, Cognetta AB 3rd, Niphakis MJ, Cravatt BF. Proteome-wide reactivity profiling identifies diverse carbamate chemotypes tuned for serine hydrolase inhibition. *ACS Chem Biol.* 2013; 8:1590–1599. [PubMed: 23701408]

27. Speers AE, Cravatt BF. Activity-Based Protein Profiling (ABPP) and Click Chemistry (CC)-ABPP by MudPIT Mass Spectrometry. *Curr Protocol Chem Biol.* 2009; 1:29–41.
28. Wiekowski MR, Giorgi C, Lebedzinska M, Duszynski J, Pinton P. Isolation of mitochondria-associated membranes and mitochondria from animal tissues and cells. *Nat Protocols.* 2009; 4:1582–1590. [PubMed: 19816421]
29. Suzuki J, Kanemaru K, Ishii K, Ohkura M, Okubo Y, Iino M. Imaging intraorganellar Ca²⁺ at subcellular resolution using CEPIA. *Nat Commun.* 2014; 5:4153. [PubMed: 24923787]
30. Teramoto S, Tomita T, Matsui H, Ohga E, Matsuse T, Ouchi Y. Hydrogen peroxide-induced apoptosis and necrosis in human lung fibroblasts: protective roles of glutathione. *Jpn J Pharmacol.* 1999; 79:33–40. [PubMed: 10082315]
31. Hampton MB, Orrenius S. Dual regulation of caspase activity by hydrogen peroxide: implications for apoptosis. *FEBS Letters.* 1997; 414:552–556. [PubMed: 9323034]
32. Baines CP, Kaiser RA, Purcell NH, Blair NS, Osinska H, Hambleton MA, Brunskill EW, Sayen MR, Gottlieb RA, Dorn GW, Robbins J, Molkentin JD. Loss of cyclophilin D reveals a critical role for mitochondrial permeability transition in cell death. *Nature.* 2005; 434:658–662. [PubMed: 15800627]
33. Cravatt BF, Wright AT, Kozarich JW. Activity-based protein profiling: from enzyme chemistry to proteomic chemistry. *Ann Rev Biochem.* 2008; 77:383–414. [PubMed: 18366325]
34. Kambe T, Correia BE, Niphakis MJ, Cravatt BF. Mapping the protein interaction landscape for fully functionalized small-molecule probes in human cells. *J Amer Chem Soc.* 2014; 136:10777–10782. [PubMed: 25045785]
35. Adibekian A, Martin BR, Wang C, Hsu KL, Bachovchin DA, Niessen S, Hoover H, Cravatt BF. Click-generated triazole ureas as ultrapotent *in vivo*-active serine hydrolase inhibitors. *Nat Chem Biol.* 2011; 7:469–478. [PubMed: 21572424]
36. Sun FC, Wei S, Li CW, Chang YS, Chao CC, Lai YK. Localization of GRP78 to mitochondria under the unfolded protein response. *Biochem J.* 2006; 396:31–39. [PubMed: 16433633]
37. Poderoso C, Converso DP, Maloberti P, Duarte A, Neuman I, Galli S, Cornejo Maciel F, Paz C, Carreras MC, Poderoso JJ, Podesta EJ. A mitochondrial kinase complex is essential to mediate an ERK1/2-dependent phosphorylation of a key regulatory protein in steroid biosynthesis. *PLoS One.* 2008; 3:e1443. [PubMed: 18197253]
38. Gelb MH, Svaren JP, Abeles RH. Fluoro ketone inhibitors of hydrolytic enzymes. *Biochemistry.* 1985; 24:1813–1817. [PubMed: 2990541]
39. Street IP, Lin HK, Laliberté F, Ghomashchi F, Wang Z, Perrier H, Tremblay NM, Huang Z, Weech PK, Gelb MH. Slow- and tight-binding inhibitors of the 85-kDa human phospholipase A₂. *Biochemistry.* 1993; 32:5935–5940. [PubMed: 8018213]
40. Barbayanni E, Stephens D, Grkovich A, Magrioti V, Hsu YH, Dolatzas P, Kalogiannidis D, Dennis EA, Kokotos G. 2-Oxoamide inhibitors of phospholipase A₂ activity and cellular arachidonate release based on dipeptides and pseudodipeptides. *Bioorg Med Chem.* 2009; 17:4833–4843. [PubMed: 19443224]
41. Long JZ, Cisar JS, Milliken D, Niessen S, Wang C, Trauger SA, Siuzdak G, Cravatt BF. Metabolomics annotates ABHD3 as a physiologic regulator of medium-chain phospholipids. *Nat Chem Biol.* 2011; 7:763–765. [PubMed: 21926997]
42. Savinainen JR, Saario SM, Laitinen JT. The serine hydrolases MAGL, ABHD6 and ABHD12 as guardians of 2-arachidonoylglycerol signalling through cannabinoid receptors. *Acta Physiologica.* 2012; 204:267–276. [PubMed: 21418147]
43. Kamat SS, Camara K, Parsons WH, Chen DH, Dix MM, Bird TD, Howell AR, Cravatt BF. Immunomodulatory lysophosphatidylserines are regulated by ABHD16A and ABHD12 interplay. *Nat Chem Biol.* 2015; 11:164–171. [PubMed: 25580854]
44. Lin DT, Conibear E. ABHD17 proteins are novel protein depalmitoylases that regulate N-Ras palmitate turnover and subcellular localization. *eLife.* 2015; 4:e11306. [PubMed: 26701913]
45. Naresh Kumar M, Thunuguntla VBSC, Veeramachaneni GK, Chandra Sekhar B, Guntupalli Swapna, Bondili JS. Molecular characterization of human ABHD2 as TAG lipase and ester hydrolase. *Biosci Rep.* 2016; 36:e00358. [PubMed: 27247428]

46. Miller MR, Mannowetz N, Iavarone AT, Safavi R, Gracheva EO, Smith JF, Hill RZ, Bautista DM, Kirichok Y, Lishko PV. Unconventional endocannabinoid signaling governs sperm activation via the sex hormone progesterone. *Science*. 2016; 352:555–559. [PubMed: 26989199]
47. Ding X, Yang J, Wang S. Antisense oligonucleotides targeting abhydrolase domain containing 2 block human hepatitis B virus propagation. *Oligonucleotides*. 2011; 21:77–84. [PubMed: 21466387]
48. Xia W, Shen Y, Xie H, Zheng S. Involvement of endoplasmic reticulum in hepatitis B virus replication. *Virus Res*. 2006; 121:116–121. [PubMed: 16870295]
49. Geng X, Huang C, Qin Y, McCombs JE, Yuan Q, Harry BL, Palmer AE, Xia NS, Xue D. Hepatitis B virus X protein targets Bcl-2 proteins to increase intracellular calcium, required for virus replication and cell death induction. *Proc Natl Acad Sci USA*. 2012; 109:18471–18476. [PubMed: 23091012]
50. Bachovchin DA, Cravatt BF. The pharmacological landscape and therapeutic potential of serine hydrolases. *Nat Rev Drug Discov*. 2012; 11:52–68. [PubMed: 22212679]
51. Niphakis MJ, Cravatt BF. Enzyme inhibitor discovery by activity-based protein profiling. *Ann Rev Biochem*. 2014; 83:341–377. [PubMed: 24905785]

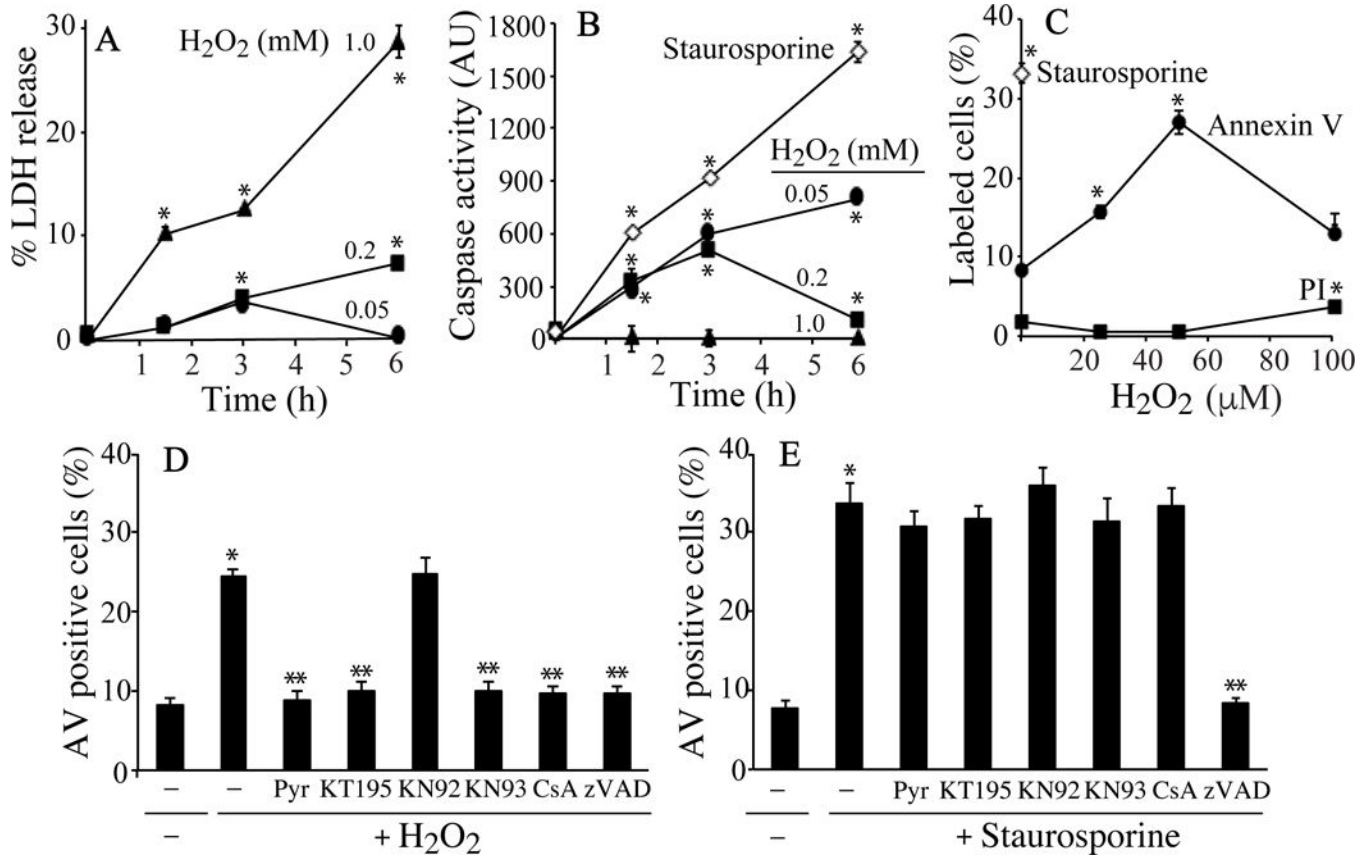


Fig. 1. H₂O₂ induces apoptosis and necrosis in MLF

LDH release (A) and caspase activity (B) were determined in MLF treated with H₂O₂ (0.05, 0.2, and 1.0 mM) or staurosporine (250 nM) for the indicated times. Caspase activity is expressed as arbitrary units (AU) of fluorescence intensity. MLF were stained for annexin V (AV) and propidium iodide (PI) after stimulation with the indicated concentrations of H₂O₂ or staurosporine (250 nM) (C). MLF were also stained for AV after pre-incubation with pyrrophenone (Pyr, 2 μM), KT195 (2 μM), KN93 (10 μM), KN92 (control, 10 μM), Cyclosporine A (CsA, 10 μM), and zVAD (20 μM) for 30 min followed by stimulation with H₂O₂ (50 μM) (D) or staurosporine (250 μM) (E) for 6 hr. The results are the average of three independent experiments (n=3, ±S.E. *P<0.05 compared to unstimulated controls, **P<0.05 compared to stimulated cells without inhibitors).

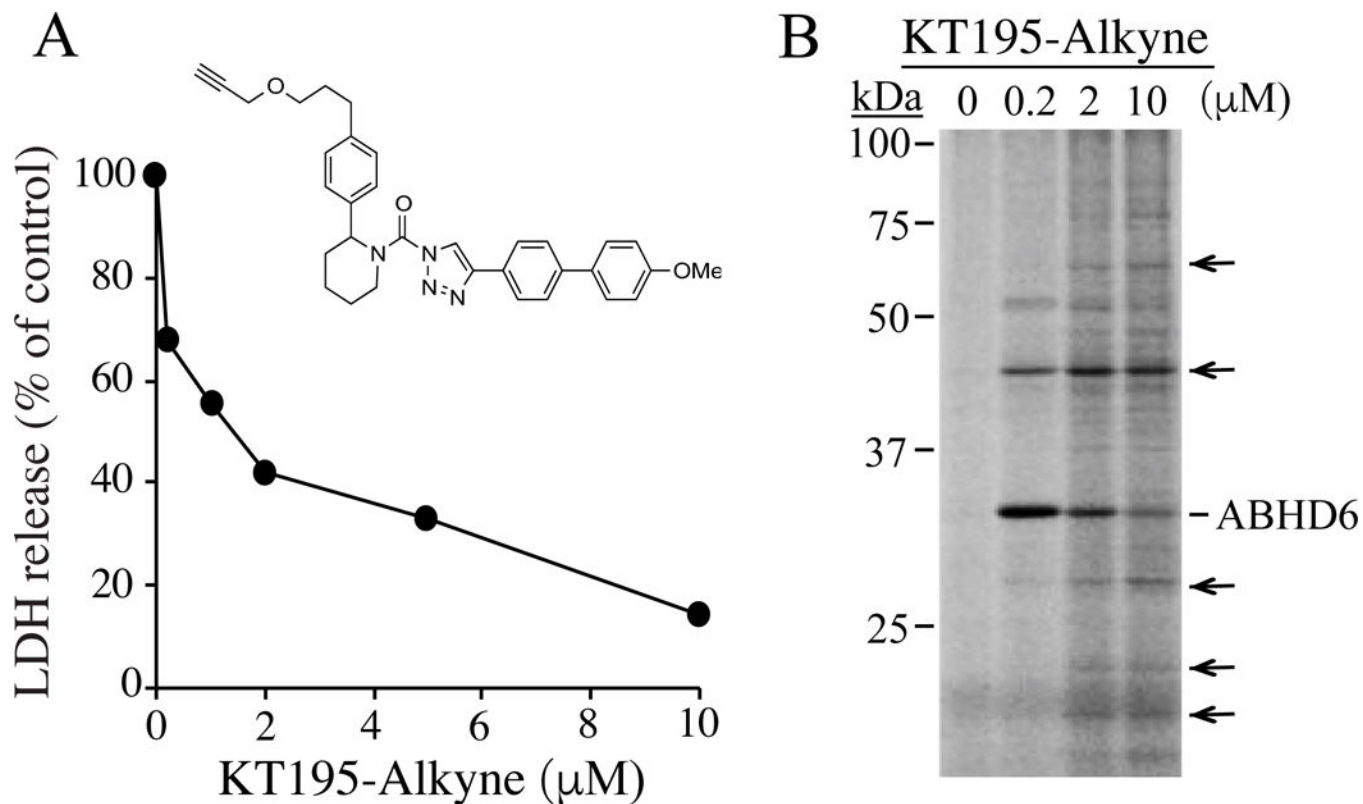


Fig. 2. KT195-alkyne inhibits cell death and labels protein targets

(A) IMLF treated with KT195-alkyne were stimulated with A23187 (1 $\mu\text{g}/\text{ml}$) for 30 min and LDH release was determined. (B) Membrane proteomes were prepared from IMLF treated with KT195-alkyne (0, 0.2, 2, and 10 μM) then click chemistry carried out with Rhodamine-azide. Rhodamine-labeled proteins were separated on SDS-polyacrylamide gels and visualized by in-gel fluorescence scanning.

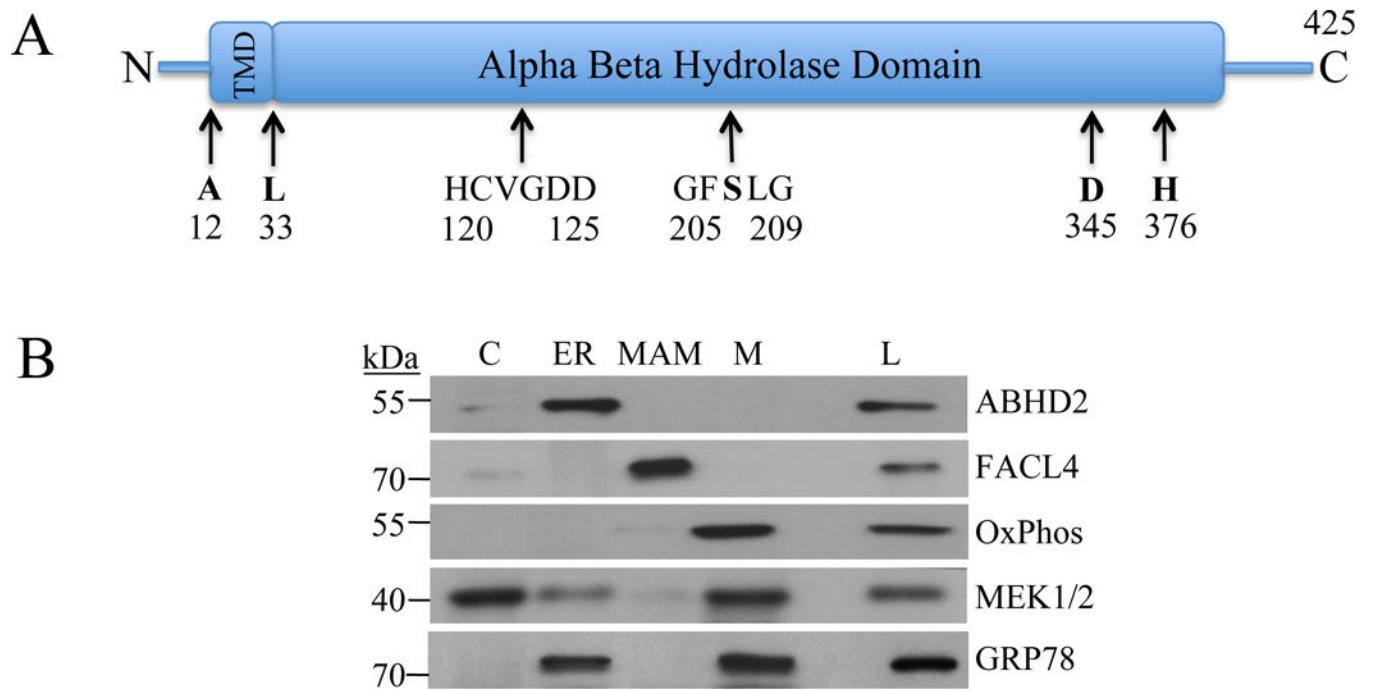


Fig. 3. ABHD2 localizes to the ER

Subcellular fractions (cytosol (C), ER, MAM, mitochondria (M)) and whole cell lysates (L) were prepared from IMLF and analyzed for protein markers by Western blot analysis using antibodies to ABHD2, fatty acid CoA ligase 4 (FACL4), oxidative phosphorylation complex V (OxPhos), MEK1/2 and GRP78.

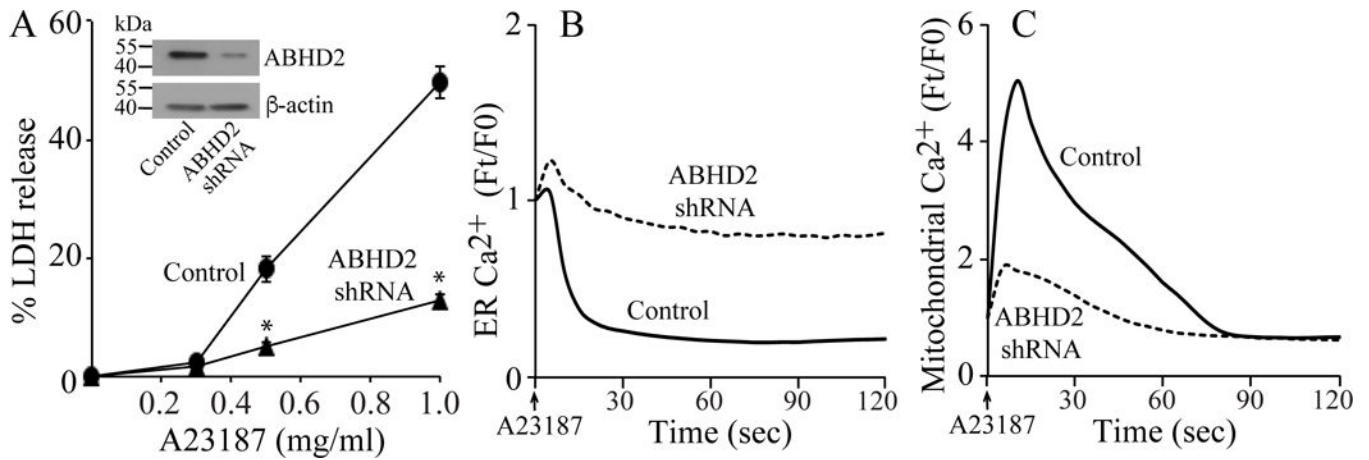


Fig. 4. ABHD2 Knockdown attenuates cell death and calcium transfer from ER to mitochondria
 IMLF were transfected with lentiviruses containing ABHD2 shRNA or control vector and stable clones generated. (A) LDH release was measured from ABHD2 shRNA-knockdown IMLF (triangles) and vector controls (circles) 30 min after stimulation with the indicated concentrations of A23187 (n=3, *P<0.05). A Western blot (inset) shows that ABHD2 shRNA-knockdown IMLF express less ABHD2 than vector controls. G-CEPIA_{er} or CEPIA_{mt} was expressed in vector control (solid line) and ABHD2 shRNA-knockdown IMLF (hatched line) to measure relative changes in ER (B) and mitochondrial (C) calcium, respectively. Calcium transients were measured after addition of A23187 (1 μ g/ml) by live-cell fluorescent imaging. The data represent the average of three independent experiments from analysis of at least 5 cells/experiment.

Table 1

Proteins identified as targets of KT195

Number of Experiment	Exp 1		Exp 2		Exp 3	
	none	none	KT195	none	none	Pyr
Protein Candidates						
	Number of peptides					
ABHD6	16	23	0	17	20	
Neutral cholesterol ester hydrolase	8	4	3	8	9	
Lysosomal protective protein	4	0	2	5	2	
Group XV phospholipase A2	2	3	0	4	4	
ABHD11	3			4	3	
Retinoid-inducible serine carboxypeptidase	2	0	1	2	2	
Acyl-protein thioesterase 2	1			1	1	
ADP/ATP translocase 2	1	0	1	1	2	
Platelet activating factor acetylhydrolase	1			1	2	
ABHD2	1	3	0	1	0	
Non-specific lipid-transfer protein	4	1	4	1	2	

The numerical values correspond to the number of tryptic peptides identified by LC-MS for each protein that was recovered in biotin-azide pull-down experiments from membrane proteomes of IMLF treated with KT-195 alkylne. In competition experiments IMLF were pretreated with KT195 (Exp 2) or pyrrophenone (Exp 3) prior to treatment with KT195-alkylne.